How to include frequency dependent complex permeability Into SPICE models to improve EMI filters design?

Fabien Sixdenier, Ousseynou Yade, Christian Martin, Arnaud Bréard, Christian Vollaire

How to include frequency dependent complex permeability Into SPICE models to improve EMI filters design?

Fabien Sixdenier, Ousseynou Yade, Christian Martin, Arnaud Bréard, and Christian Vollaire

Citation: AIP Advances **8**, 056604 (2018);
View online: https://doi.org/10.1063/1.5004630
View Table of Contents: http://aip.scitation.org/toc/adv/8/5
Published by the American Institute of Physics

How to include frequency dependent complex permeability Into SPICE models to improve EMI filters design?

Fabien Sixdenier,[1,a] Ousseynou Yade,[2] Christian Martin,[1] Arnaud Bréard,[2] and Christian Vollaire[2]
[1]*Univ Lyon, UCB Lyon 1, CNRS, AMPERE, Villeurbanne F-69100, France*
[2]*Univ Lyon, ECL, CNRS, AMPERE, Villeurbanne F-69134, France*

(Presented 7 November 2017; received 14 September 2017; accepted 16 October 2017; published online 7 December 2017)

Electromagnetic interference (EMI) filters design is a rather difficult task where engineers have to choose adequate magnetic materials, design the magnetic circuit and choose the size and number of turns. The final design must achieve the attenuation requirements (constraints) and has to be as compact as possible (goal). Alternating current (AC) analysis is a powerful tool to predict global impedance or attenuation of any filter. However, AC analysis are generally performed without taking into account the frequency-dependent complex permeability behaviour of soft magnetic materials. That's why, we developed two frequency-dependent complex permeability models able to be included into SPICE models. After an identification process, the performances of each model are compared to measurements made on a realistic EMI filter prototype in common mode (CM) and differential mode (DM) to see the benefit of the approach. Simulation results are in good agreement with the measured ones especially in the middle frequency range. https://doi.org/10.1063/1.5004630

I. INTRODUCTION

Static converters have made a lot of progress these last decades thanks to a better knowledge of semiconductor power switches and the increase of switching frequencies which allows to reduce drastically the volume of passive components (magnetic, and capacitors). Unfortunately, increasing the switching frequency leads to generate a large amount of electromagnetic interferences (EMI). Two types of disturbances exist: common mode (CM) and differential mode (DM). Usually, each type of disturbance requires a specific magnetic component (an inductance designed with winding modes and materials well suited to every need) and specific capacitors (Cx(DM),Cy(CM)). Scientists and engineers are then involved in the development of EMI filters design softwares.[1,2] These approaches generally neglect the frequency dependent complex permeability (μ) of the soft magnetic materials (with $\mu(f) = \mu'(f) - j\mu''(f)$). The real part μ' gives an image of how much energy can be stored whereas μ'' gives an image of the losses. Two frequency-dependent complex permeability models able to be included into SPICE models for AC analysis are presented here. The first model is inspired by the magnetic field diffusion equation solution[3] and the second one is inspired by Nomura's work.[4] Both models are implemented thanks to behavioural sources and Laplace equations available in Spice softwares. Their implementation in LTSpice®will be explained in the second section. Results concerning the ability of each model to predict complex permeability versus frequency on two different materials will be shown on the third section as well as all simulation cases of the EMI filter to see the benefits of the approach on a realistic device. Discussion of all the results will be made in the fourth section. The last section will summarize the

[a]Electronic mail: fabien.sixdenier@univ-lyon1.fr

results and propose some prospects about using this approach in a future complete filter design tool.

II. COMPLEX PERMEABILITY MODELS AND IMPLEMENTATION IN SPICE

Due to their excellent magnetic properties (low losses, high μ_r and high B_s), nanocrystalline materials became more suitable for common mode inductors than laminated or powder iron and ferrites.[5] In our case, we chose, for our EMI filter prototype, Nanophy[6] cores ($\mu_r \approx 30000$) for CM and $K\mu$[6] ($\mu_r \approx 200$) cores for DM. Real and imaginary parts of complex permeability were extracted from impedance measurements made on each core thanks to an HP4294A impedance analyser.[7] These measurements were, then, taken as reference to fit both models.

A. Complex permeability models

1. Diffusion's like model

As nanocrystalline alloys have a relatively high electrical conductivity ($\sigma \approx 833$ kS/m), skin effect will necessary occur, even if the layers thickness is very low (≈ 18 μm). Starting from the diffusion equation, the complex permeability μ can be expressed like (1),[3] where ω_0 is the pulsation where the skin depth is equal to the half thickness of the strip and μ_{DC} is the low frequency value of μ'. Only 2 parameters per material have to be identified with this model.

$$\mu = \mu_{DC} \frac{\tanh \sqrt{\frac{j\omega}{\omega_0}}}{\sqrt{\frac{j\omega}{\omega_0}}} \tag{1}$$

2. Nomura's model

Nomura[4] proposed a model that used two straight lines on a log-log plot via a generic equation (2) able to describe μ' or μ'' versus frequency.

$$\mu(f) = \frac{10^{a_2 \log_{10}(f)+b_2}}{1 + 10^{(a_2-a_1)\log_{10}(f)+(b_2-b_1)}} \tag{2}$$

a_1, a_2 are the slopes and b_1 and b_2 are y intercepts of each line respectively. Thus, for a given material, we had to identify 4 parameters per curve (μ' and μ'') so 8 parameters in total. These parameters were fitted numerically for better accuracy.

B. LTSPICE implementation

For both models implementation, a gyrator[8,9] was used in order to separate electrical and magnetic physical domains. With this analogy, magneto-motive forces and flux time derivative (in AC analysis the flux time derivative $d\phi/dt$ becomes $j\omega\phi$) became equivalent to voltages and currents respectively. Both models implementation required current controlled voltage sources, behavioural voltage sources, spice directives and mathematical functions expressed in function of the Laplace operator ($s = j\omega$) instead of the frequency f.

1. Diffusion's like model

The figure 1 shows an example of a single winding and a single magnetic circuit. In figure 1, $B1$ and $B2$ are current controlled voltage sources that represent the winding and the coupling between electrical and magnetic physical domains (gyrator). The behavioural source *B_Re_mu* represents the magnetic circuit (A_e is the magnetic circuit cross section, *MPL* is the average magnetic path length and μ_0 is the vacuum permeability). One can also see in figure 1, how (1) is programmed with a *.func* SPICE directive. The other equation calculates the complex reluctance $\mathfrak{R}$ as (3). It has to be mentioned that resistors $R3$ and $R1$ are fictitious resistors inserted here, in order to avoid to have only pure voltage sources linked in a current loop.

$$\mathfrak{R} = \frac{1}{\mu_0 \mu} \cdot \frac{MPL}{A_e} \tag{3}$$

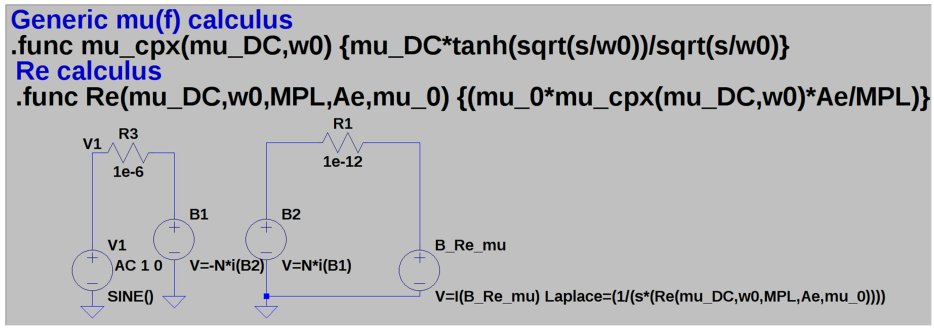

FIG. 1. Diffusion's like model implementation in LTSPice.

2. *Nomura's model implementation*

Nomura[4] used behavioural voltage sources (*bvs*) to reproduce the resistive and inductive behaviour of the total impedance of a common mode choke. In our case, the electrical inductive and resistive behaviours are modeled by using in the magnetic domain a capacitor (C_μ) and a resistor (R_μ) respectively[10] linked in series.

$$C_\mu = \frac{\mu_0 A_e(\mu'^2 + \mu''^2)}{\mu' MPL} \tag{4}$$

$$R_\mu = \frac{\mu'' MPL}{\mu_0 \omega A_e(\mu'^2 + \mu''^2)} \tag{5}$$

To sum up, the Nomura's model needs two coupled current controlled voltage sources to represent the winding through a gyrator) and two behavioural sources to represent R_μ and C_μ. Calculations of (2), (4), (5) are made via SPICE directives as explained before.

III. RESULTS

A. Material models results

The Nanophy and $K\mu$ materials were characterized and the parameters of the both models were identified by numerically fitting the simulated curves with respect to the measured ones. Nomura and diffusion's like model parameters are listed in Table I.

The figure 2 shows the real and imaginary parts of complex permeability computed by both models compared to measurements for high (Nanophy) and low (Kμ) permeability cores. The shape of each curve is globally retrieved by both models. Nevertheless, one can see that (1) is limited in

TABLE I. Nomura and diffusion's like model parameters.

Nanophy cores ($\mu_r \approx 30000$)							
	Nomura's model					diffusion's like model	
	a_1	a_2	b_1	b_2		μ_{DC}	ω_0 (rad/s)
μ'	−0.0116	−1.1483	4.6099	10.30	μ	35023	1.99e5
μ''	0.5303	−0.8063	1.5041	8.368			
Kμ cores ($\mu_r \approx 200$)							
	Nomura's model					diffusion's like model	
	a_1	a_2	b_1	b_2		μ_{DC}	ω_0 (rad/s)
μ'	0.0003	−1.56	2.356	13.84	μ	226	4.429e7
μ''	1.0054	−0.627	−5.29	6.745			

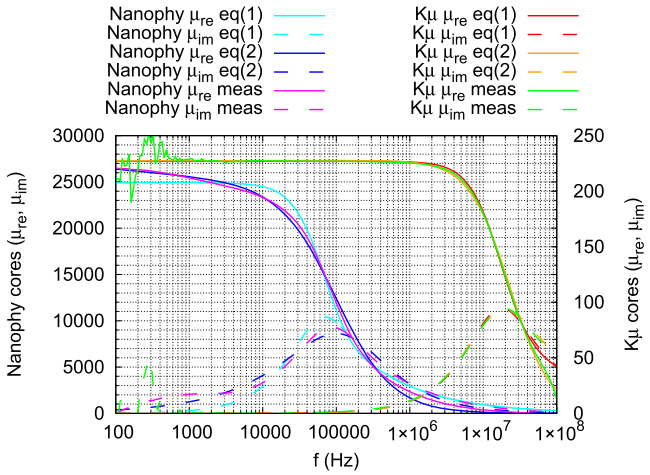

FIG. 2. Real μ_{re} and imaginary μ_{im} parts of complex permeability computed by diffusion's like model (1), Nomura's model (2) and comparison with measurements for Nanophy cores (left axis) and Kμ cores (right axis).

terms of accuracy compared to (2) especially for Nanophy cores in the whole frequency range. Other tests (not shown) made on materials with permeabilities μ_r ≈3000, μ_r ≈30000 and μ_r ≈500000 confirmed this tendency. So far, the only drawback of Nomura's model is that it has more parameters to identify than the diffusion's like model (8 versus 2 respectively). The identification process is then a bit more difficult and takes more time.

B. EMI filter prototype

The figure 3 shows the EMI filter scheme with common mode and differential excitation sources connections to test one or other mode. EMI filters nominal values for each component are listed in the Table II

The input impedance of this filter will be measured and the results will be be compared to 4 simulation cases, listed in the Table III, in each mode (common and differential) for each model.

Equivalent serial R, L, C values for C_x and C_y capacitors (used for simulation cases B to D) are listed in the Table IV. In the same table are reported the dimensions and number of turns of each inductor (simulation cases C and D).

Impedance modulus and argument have been measured and simulated (4 cases) with the proposed models. Impedance modulus in common and differential modes are plotted in figures 4 and 5 respectively. Discussion about the results is on the next section.

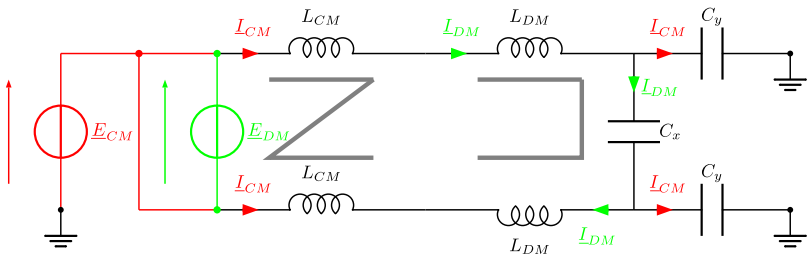

FIG. 3. EMI filter scheme with common mode (red) and differential (green) excitation sources connections.

TABLE II. EMI filter needed values.

L_{CM} (mH)	L_{DM} (μH)	C_x (nF)	C_y (nF)
5.7	40	100	4.7

TABLE III. Simulation cases details.

Case	Details
A	all capacitors and inductors are ideal
B	capacitors are replaced by R,L,C serial model
C	Inductors are replaced by diffusion's like or Nomura's models
D	same as case C, plus parasitic capacitances in parallel of each winding.

TABLE IV. Equivalent serial *ESR*, *ESL*, *C* values for C_x and C_y and core dimensions and number of turns for L_{CM} and L_{DM}.

	ESR (mΩ)	*ESL* (nH)	*C* (nF)
C_x	76.5	54	98.5
C_y	330	43.6	4.83
	MPL (mm)	A_e (mm^2)	*N* (turns)
L_{CM}	61.3	14.62	25
L_{DM}	60.8	13.41	26

IV. DISCUSSION

First, one can observe that cases "A" and "B" are quite the same. Indeed, self-resonance frequencies of C_x and C_y are very high ($f_{C_x} \approx 2.2$ MHz, $f_{C_y} \approx 10$ MHz) and *ESL* values are very low compared to L_{CM} or L_{DM}, so their influence on the impedance modulus in any mode is negligible. The benefits of our approach can be clearly seen in figure 4, when 40 kHz $< f <$ 10 MHz because simulated cases "C" and "D" are in far better agreement with measurements than the cases "A" and "B". This is mainly due to Nanophy cores μ' and μ'' large variations in this frequency range (see figure 2). As the complex permeability was better predicted with Nomura's model (2) than with the diffusion's like model (1) (see figure 2), the results obtained on the EMI filter (see figures 4) of cases "C" or "D" are better when using (2) than (1) in the filter SPICE model. In differential mode (figure 5), the K_μ ($\mu_r = 200$) core is solicited. For this core μ' and μ'' are relatively stable until 2 MHz. That's why all simulation cases (even ideal ones) are in good agreement with experimental results. No model seems better than the other for DM mode. By connecting on each winding, of each core, a parasitic capacitance $C_p = 8$ pF (fitted after a complete EMI filter measurement), the simulated second resonance peaks (curves of Cases "D") in each mode are in good agreement with the measurements. The third and fourth measured resonance peaks ($f >$ 10 MHz) are certainly due to turn to shield

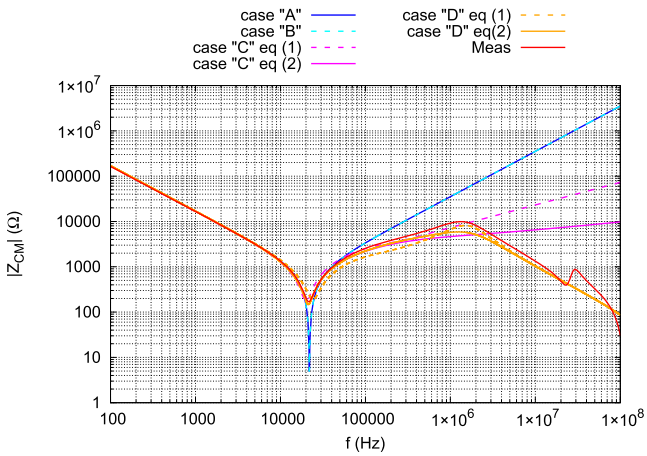

FIG. 4. Impedance modulus results in common mode excitation for all simulation case and both models.

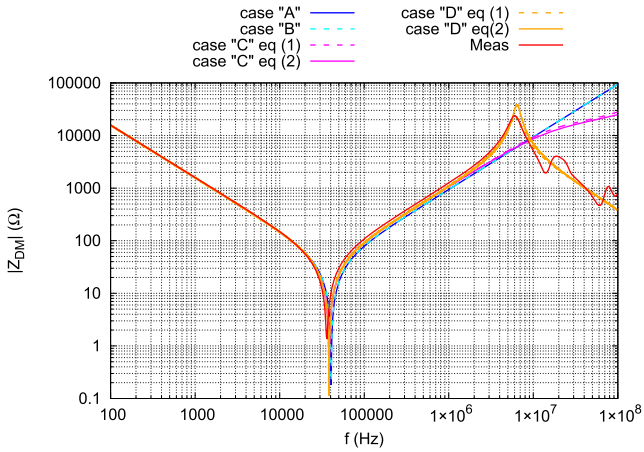

FIG. 5. Impedance modulus results in differential mode excitation for all simulation case and both models.

capacitances[11] that are resonating with stray inductances (connections mainly). To predict these very high resonance peaks, accurate numerical tools should be employed and are therefore out of the scope of this study.

V. CONCLUSION

Two analytical models able to predict the frequency dependent magnetic complex permeability behaviour were analysed in this paper. After identification, Nomura's model showed that it has a better accuracy in the whole frequency range and is more robust (better adaptability to various materials). Nomura's model seems to be a better choice even if it is a bit more difficult to identify. This tendency has to be confirmed by further work on other materials like ferrite or iron powders. Both models have been successfully implemented in LTSpice® thanks to the tools available in the software, to simulate a realistic EMI filter. Both models showed that it is crucial to take into account the frequency dependant properties of magnetic material in the medium frequency range especially in common mode. Adding a parasitic capacitance on each winding allowed to retrieve the second resonance peak in both modes. Unfortunately, its value is very hard to predict analytically.[11] That's why Future work will focus on this task in order to have a full design tool accurate enough to do EMI filter virtual prototyping.

ACKNOWLEDGMENTS

This project has received funding from the European Union's Horizon 2020 research and innovation programme under grant agreement N° 636170.

[1] C. Henkenius, N. Fröhleke, and J. Böcker, "Numerical optimization of passive line filter components for suppression of electromagnetic interference (EMI)," in *Applied Power Electronics Conference and Exposition (APEC), 2016 IEEE* (IEEE, Long Beach, CA, USA, 2016).
[2] B. Narayanasamy, H. Jalanbo, and F. Luo, "Development of software to design passive filters for EMI suppression in SiC DC fed motor drives," in *Wide Bandgap Power Devices and Applications (WiPDA), 2015 IEEE 3rd Workshop on* (IEEE, Blacksburg, VA, USA, 2015).
[3] *Induction Machines* (Taylor & Francis, 1995).
[4] K. Nomura, N. Kikuchi, Y. Watanabe, S. Inoue, and Y. Hattori, "Novel spice model for common mode choke including complex permeability," in *2016 IEEE Applied Power Electronics Conference and Exposition (APEC)* (2016) pp. 3146–3152.
[5] A. Roch and F. Leferink, "Nanocrystalline core material for high-performance common mode inductors," IEEE Transactions on Electromagnetic Compatibility **54**, 785–791 (2012).
[6] "APERAM," .
[7] "Hp4294a datasheet," .
[8] D. C. Hamill, "Lumped equivalent circuits of magnetic components: The gyrator-capacitor approach," IEEE Transactions on Power Electronics **8**, 97–103 (1993).
[9] D. C. Hamill, "Gyrator-capacitor modeling: A better way of understanding magnetic components," in *Applied Power Electronics Conference and Exposition, 1994. APEC '94. Conference Proceedings 1994., Ninth Annual* (1994) pp. 326–332 vol. 1.

[10] F. Mesmin, F. Sixdenier, H. Chazal, and A. Kedous-Lebouc, "Improvement of EMI filters performance by taking into account frequency-dependant magnetic material properties," in *Proceedings of the 18th Conference on the Computation of Electromagnetic Fields* (Compumag 2011, Sydney : Australia, 2011).

[11] G. Grandi, M. K. Kazimierczuk, A. Massarini, and U. Reggiani, "Stray capacitances of single-layer air-core inductors for high-frequency applications," in *Industry Applications Conference, 1996. Thirty-First IAS Annual Meeting, IAS '96., Conference Record of the 1996 IEEE*, Vol. 3 (1996) pp. 1384–1388 vol. 3.